Edinburgh Research Explorer

The effect of pore structure on the CO2 adsorption efficiency of polyamine impregnated porous carbons

OPEN ACCESS

The effect of pore structure on the CO_2 adsorption efficiency of polyamine impregnated porous carbons

J. A. Arran Gibson[a,b]*, Andrei V. Gromov[a], Stefano Brandani[b] and Eleanor E.B. Campbell[a,c]

[a] EaStCHEM, School of Chemistry, University of Edinburgh, Edinburgh, UK
[b] SCCS, School of Engineering, The University of Edinburgh, Edinburgh, UK
[c] Division of Quantum Phases and Devices, Konkuk University, Seoul 143-701, Korea

Abstract

The effect of polyamine impregnation on the CO_2 adsorption properties of two different porous carbons, one microporous and one mesoporous, was studied systematically. The pore filling during impregnation with polyamines was shown to result in a fraction of the unfilled micropore volume being blocked for gas adsorption. Thermal gravimetric analysis was used to compare the CO_2 capacity at 0.1 bar with respect to the carbon support type, the amount of amine loading, and the type of amine. A 12 fold increase in the CO_2 capacity was observed when the impregnated activated carbon was compared to the raw starting material. A heat of adsorption for amine impregnated support of ~90 kJ mol^{-1} was found, clearly indicating a chemisorption mechanism. The mesoporous material provided a more efficient support for the amine to interact with the CO_2. The interaction between low molecular weight amines and CO_2 showed a more efficient utilization of the basic groups in comparison to high molecular weight species.

Graphical Abstract
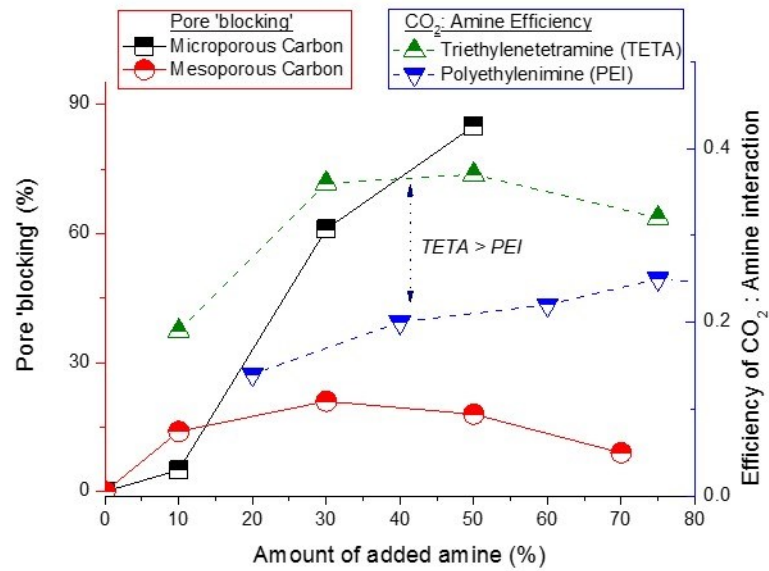
Highlights

- A study of two carbons, one microporous and one mesoporous, impregnated with amines.
- Larger pores enable a more efficient interaction between CO2 and impregnated amine.
- Lower molecular weight amines interact more efficiently with CO2 during adsorption.
- Amine impregnation blocked a fraction of the micropore volume for gas adsorption.

1. Introduction

Recent environmental concerns regarding world CO_2 emissions have driven research into the development of novel adsorbents for the deployment of carbon capture and storage (CCS). There are two main processes being considered for CCS, adsorption and absorption, the advantages and disadvantages of both processes are discussed in a review by Yu et al.[1] For adsorption to be feasible in a post-combustion process, materials that have a high CO_2 capacity, are highly selective and stable need to be developed.

Activated carbon is a versatile adsorbent material widely used in gas adsorption/separation as well as for waste water treatment.[2-5] Due to its highly developed surface (micro/mesoporous structure) and availability, activated carbon is considered as a relatively low-cost solid adsorbent in CO_2 capture and separation applications. However, the selectivity of CO_2/N_2 separation is fairly moderate[6] and therefore it is considered to be practical only for CO_2 rich gas mixtures (i.e. pre-combustion capture)[7, 8]. Surface modification of activated carbon with impregnated organic basic moieties was reported to improve the selectivity of activated carbon and improve the total capacity with respect to CO_2 due to the change of the adsorption mechanism from physisorption to chemisorption[9-13] . This should ensure CO_2 uptake even from CO_2 dilute gas mixtures(i.e flue gas). However, literature results vary significantly depending on the amine/carbon substrate and the conditions and procedure used to calculate the CO_2 capacity. For example, recent results show a capacity of up to 1.5 mmol g^{-1} for monoethanolamine [10] and 1.1 mmol g^{-1} for polyethylenimine (PEI) impregnated microporous activated carbons[14]. For mesoporous carbon impregnated with PEI, Wang et al reported a CO_2 capacity of up to 5 mmol g^{-1} at a high CO_2 partial pressure[11]. The majority of the work, to date, on this approach is covered in a few comprehensive reviews on the properties of solid sorbents for carbon capture[6, 13, 15].

The alternative solid support material to porous carbons is mesoporous silica. There are a large number of promising reports in the literature on the potential of silicas loaded with a variety of amines.[15-24] A recent paper by Wang et al. [25] compared different mesoporous silicas and emphasized the importance of pore structure for efficient utilization of amine on the support. However, there is a difference in terms of the loading of the amine onto the carbon support, as the cohesive properties of the silica and carbon surfaces will vary [2, 26, 27]. One advantage of carbon supports over the related silica materials is the potential of thermal regeneration of the adsorbent bed through ohmic heating[28].

In spite of the plethora of studies, there is still a lack of information concerning the effect of surface impregnation on the porosity and surface structure of the activated carbon materials. There have been some suggestions in the literature concerning the optimum level of impregnation required to achieve the highest CO_2 capacity[11, 15], however, the value appears to be highly dependent on the nature and structure of the support. In some cases difficulties were reported in loading more than a small weight percentage of amine onto the support. [12, 29] This however appears to be a result of the choice of the material and it would seem that the success of the impregnation depends on the morphology of the support. There have been conflicting reports on how large an effect impregnating activated carbon with amine has on the CO_2 capacity of the adsorbent. For example, Arou et al [29] impregnated a microporous carbon with polyethyleneimine (PEI) and observed that a weight loading of PEI greater than 0.26 wt% had a detrimental effect on the CO_2 capacity. In contrast, a study by Lee et al[9] into the use of sterically hindered amines impregnated (40 wt%) on palm shell derived activated carbon reported a significant (88%) increase in the enhancement in the CO_2 capacity despite a large reduction in the accessible surface area. In this work we provide insight into some of the reasons behind the contrasting results in the literature by directly and systematically comparing two carbons with different pore structures. The discussion is then advanced to examine how efficiently the active sites are utilized on the support and how the molecular weight of the amine impacts on its reactivity towards CO_2.

One major limitation of solid supports impregnated with low molecular weight amine derivatives is their low stability and performance over repeated adsorption and desorption cycles.[9, 30] The relative potential and stability of the adsorbents over several cycles was assessed. Grafting of amines to the surface of a solid support has been suggested as a viable more stable alternative to physical impregnation of amines. [17, 31-34] Two such works include the grafting of halogenated amines on the surface of a microporous carbon by Houshmand et al.[35] and the modification of carbon powders with aminophenyl and aryl-aliphatic amine groups by Grondein et al.[31] However, the relative enhancement in the CO_2 uptake, when compared to the unmodified starting porous materials, is often more moderate than in the material prepared by impregnation.[15].

In this study we report on the impregnation of amine molecules with various molecular weights into two different porous carbon materials with different pore structures and pore size distributions. We investigate the effect of the different weight loadings of amine on the available pore volume, surface area and pore size distribution to determine the relationship between the CO_2 uptake and the morphology of the amine impregnated activated carbon.

In order to simulate post-combustion capture conditions all experiments in this study were carried out at a 0.1 bar partial pressure of CO_2. This is in the range of partial pressures that is found in the flue gas of fossil fuel power stations.

2. Experimental

2.1 Materials:

1,2-Diaminoethane anhydrous, laboratory grade reagent (further denoted as EDA) was purchased from Fisher Scientific; diethylenetriamine (DETA), 99% and polyethyleneimine with molecular weight 600 (PEI600), branched, 99% were purchased from Alfa Aesar; triethylenetetramine (TETA), tech. grade, 60% of linear isomer was purchased from Acros Organics. EDA, DETA and PEI600 were used for preparation of impregnated porous carbons without additional purification; TETA was additionally purified by vacuum distillation (b.p. 118 °C/7 mbar) before use.

Granular activated carbon (SRD 10061) was provided by Calgon Carbon. This material exhibited a microporous structure (see Table 1) and is denoted as micro-AC.

Another carbon material (further denoted as meso-AC) was synthesized using a templating method with a carbon precursor on mesoporous silicagel, similar to the method reported by Bohme et al.[36]. Typically, ~3g of dry sucrose, 2.5 g of silicagel, 20 ml of distilled water and 200 µl of conc. sulphuric acid (96%) were stirred on a hotplate at a temperature of 50-60 °C until all the water had evaporated. The homogeneous dry dark mixture was heated in an oven at 100 °C for 4 h and then 160 °C for 5h. The resulting 'caramel' was annealed at 900 °C in an Ar atmosphere for 5h. The resultant carbon-silica composite was treated with 30% KOH solution at 70 °C overnight and the product was isolated by filtration. Typically the yield of carbon material was 1-1.1 g. XPS analysis showed no presence of Si in the product.

Before the impregnation with amine, the carbon materials were heat treated at 100-120 °C under vacuum for 4-5 h. This was to ensure the removal of water from the pores before impregnation. If the heat treatment was not carried out it was observed that the stability of the materials impregnated with lower molecular weight amines was reduced.

2.2 Impregnation of carbon materials

Typically, 70-100 mg of carbon material was dispersed in 5 ml of dry dichloromethane and the calculated appropriate amount of amine (10/30/50/70 parts of amine with respect to 100 parts w/w of dried carbon material) was added to this dispersion. The dispersion was sonicated in a bath for 5-

10 min and then left for a few hours; after that the dichloromethane was removed using a rotary evaporator, the product being carbon powder. The resulting weight of the products was in good agreement with the expected yields.

The following species of impregnated carbon materials were prepared for the study by nitrogen adsorption (the number after the sample name corresponds to the weight parts of amine with respect to 100 parts of carbon material): micro-AC, micro-AC-EDA(10), micro-AC-EDA(30), micro-AC-DETA(10), micro-AC-DETA(30), micro-AC-TETA(10), micro-AC-TETA(30), micro-AC-TETA(50), micro-AC-TETA(70), micro-AC-PEI600(10), micro-AC-PEI600(30), meso-AC, meso-AC-EDA(10), meso-AC-DETA(10), meso-AC-TETA(10), meso-AC-TETA(30), meso-AC-TETA(50), meso-AC-TETA(70), meso-AC-PEI600(10). The surface properties of the prepared impregnated carbon materials are summarized in Table 1. For CO_2 capture an additional series of various loadings of meso-AC-PEI600 was prepared.

2.3 Characterisation of adsorbents

N_2 adsorption isotherms were measured at 77 K on a Quantachrome NOVA 3000 instrument. All samples were regenerated in a degas station under vacuum (< 1 mbar) at up to 75 °C to remove any adsorbed species prior to analysis. The exceptions were micro-AC-EDA(10) and meso-AC-EDA(10) that were regenerated at 40 °C (<1 mbar) and micro-AC-EDA(30) that was regenerated at 70 °C (250 mbar) in order to avoid the evaporation of the EDA. This could have resulted in incomplete removal of solvent and other species from the adsorbent.

Quantachrome AsiQwin (version 3.01) software was used to calculate micro- and mesopore volume, surface area and pore size distribution (PSD) data on the basis of experimentally obtained adsorption/desorption isotherms. The estimation of micro/mesopore surface area and volume for both carbon materials was performed using the non-local density functional theory (NLDFT) for N_2 adsorption at 77K on carbon with the kernel optimized for a mixed hybrid slit/cylindrical pore geometry. This kernel assumes a slit-pore geometry for the micropores and a cylindrical pore model to describe correctly the adsorption/condensation mechanism in the mesopores (e.g. Refs. [37, 38]). It has been reported that choosing the wrong pore geometry would result in poor DFT fitting results, and thus would lead to incorrect values of the PSD and pore volume being calculated [39]. Therefore, this particular DFT kernel was chosen because it exhibited (i) the smallest fit error of DFT calculated isotherm to the experimental isotherm for pristine and low-loading impregnated carbon materials, and (ii) it provided a good match between DFT calculated total surface area and BET surface area values.

FT-IR spectra of the materials were measured on a Smiths Illuminat IR microscope equipped with Smiths Detection ATR diamond coated objective (x36 magnification). IR spectral features of carbon materials exhibited low intensity (on the level of 0.01 absorption units) and for all spectra a baseline subtraction procedure was applied. The assignment of IR spectra was performed using the atlas of infrared characteristic group frequencies [40].

2.4 CO_2 adsorption measurements

The material's CO_2 uptake was evaluated by thermal gravimetric analysis (TGA). Measurements were carried out on a Setaram Sensys Evo TGDSC instrument. A sample of 25-40 mg was packed in a platinum crucible which was counterbalanced by an identical platinum crucible that was packed with an equivalent mass of lead balls. Experiments were carried out at a variety of temperatures and at a CO_2 partial pressure of 0.1 bar. This concentration was chosen as it is in the range of the CO_2 concentration in the flue gas of fossil fuel power stations. Samples were regenerated at 90 °C under helium flow for 4-5 hours before the sample was cooled to the desired experimental temperature. After the microbalance had stabilized, the helium flow (50 cm^3 min^{-1}) was switched to a mixture of CO_2 (5 cm^3 min^{-1}) and helium (45 cm^3 min^{-1}). The change in the sample mass corresponded to the uptake of CO_2 by the sample. The capacity and heat of adsorption were then calculated. A baseline subtraction procedure was followed prior to data analysis.

3. Results and discussion

3.1 Effect of amine loading on the pore structure of carbon materials

Nitrogen adsorption measurements on the starting carbon micro-AC and meso-AC materials produced adsorption isotherms of different type (Fig. 1a, b). The adsorption isotherm of micro-AC is clearly a Type I isotherm according to IUPAC classification, typical for a microporous material[41]. In contrast, the isotherm for meso-AC is a characteristic Type IV isotherm typical of a mesoporous material. Pore size distributions (PSD) of the starting carbon materials were calculated from the experimental nitrogen adsorption isotherms using the NLDFT with the kernel optimized for hybrid slit/cylindrical pore geometry. The micro-AC material contained mainly micropores (pore width <2 nm), and *ca* 95% of the total pore volume is provided by pores that are <2.5nm in diameter (Fig. 1c). For the meso-AC material, 92% of pore volume falls within the pore size range of 3.2 -11 nm, with a PSD mean value at 5.6 nm. This corresponds well to the PSD (pore size range 4-11.5 nm) of the template silica gel determined by the NLDFT kernel for cylindrical pores (Fig 1d). As a result of the contrasting pore structures micro-AC and meso-AC allow a systematic comparison of the influence of the pore structure on the effect of impregnation on the adsorption properties.

The aim of the impregnation was to introduce as many basic amino groups to the carbon support as possible. Among polyamines with general formula $H(HNCH_2CH_2)_nNH_2$, EDA has the highest relative content of basic amino groups, which are considered to be responsible for increasing uptake of CO_2. However, EDA is a volatile species with a vapour pressure of 13 mbar at 20 °C which is a value that is 27 and 100 times higher than for DETA and TETA respectively. Therefore for initial studies TETA was chosen as the candidate for impregnation

The success of the impregnation with TETA was proved by monitoring the weight increase of the material and by infra-red spectroscopy (Fig 2). As the amine loading increases the relative intensity of the bands at 1648 cm^{-1}, N-H bending, and 1437 cm^{-1}, CH_2 scissoring, increase. The weak peaks at 1360 cm^{-1}, which appear in the impregnated samples with high amine loading, may be attributed to carbamate salt formation in air [42].

In general the impregnation of both micro-AC and meso-AC materials with different amounts of TETA resulted in a loading dependent decrease of the pore volume and surface area (see Table 1). There was no effect on the type of N_2 adsorption isotherms which remained as Type I isotherms for the micro-AC series and Type IV isotherms for the meso-AC series of impregnated materials (Fig. 1a,

b). micro-AC materials that were impregnated with a large loading of amine (micro-AC-TETA(50) and micro-AC-TETA(70)) had very low values of BET surface area and total pore volume.

The volume of added amine in the impregnated samples usually did not exceed the available pore volume of the carbon content in the impregnated materials, except for the micro-AC-TETA(70) sample, where the volume of added amine was roughly equal to the pore volume of micro-AC (Table. 1). If the extreme assumption is made that the impregnation mechanism consists of a complete and uniform pore filling[20] of the carbon material, then the expected volume available for nitrogen adsorption (V_{free}) should be equal to the difference between the total pore volume of the starting (non-impregnated) material (V_{carbon}) and the volume of the added amine (V_{TETA}) as shown in eq.1:

$$V_{free} = V_{carbon} - V_{TETA} \qquad (eq.1)$$

However, the calculated values of the total volume from the experimental N_2 adsorption isotherms are significantly lower than the value of V_{free}, calculated from eq.1. (Fig.3).This observation implies that part of the pore volume is not filled with amine, but is blocked, and this fraction of the pore volume/surface is inaccessible to nitrogen during the adsorption measurement, consistent with the results of Sanz et al.[43] for mesoporous silicas where the impregnation of amines does not necessarily result in a uniform pore filling.   Therefore, the blocked volume in the examined impregnated materials can be defined as the difference between V_{free} and the measured total pore volume after impregnation (V_{meas}). Quantification of the extent of pore blocking was performed by normalization of the blocked pore volume to the expected volume V_{free}. So, the value of 'blocking' caused by the impregnation of porous material (or % blocking, equal to 'blocking'*100%) may be expressed as shown in eq. 2:

$$'blocking' = \frac{V_{free} - V_{meas}}{V_{free}} = 1 - \frac{V_{meas}}{V_{carbon} - V_{TETA}} \qquad (eq. 2)$$

where the term $V_{meas}/(V_{carbon} - V_{TETA})$ shows the efficiency of nitrogen permeability to the available adsorption sites in the pores. Note that these considerations can only be applied to positive values of V_{free}. They cannot be applied in the case of a very low measured pore volume that could be the result of either complete pore filling with an excessive volume of impregnating species (0 or negative V_{free} values, micro-AC-TETA(70)) or the formation of a shell around the surface of the adsorbent that is non-permeable to the nitrogen at 77 K. In the latter case the material can be considered to be non-porous and its surface area and volume would derive from the particle size and interstitial voids (micro-AC-TETA(50)). For such a material an increase of amine loading, in

practice, would not change the measured BET surface area and total pore volume, but would change significantly the V_{free} value and would give misleading estimates of 'blocking' values.

In micro-AC materials the initial impregnation resulted only in insignificant pore blocking (5% in micro-AC-TETA(10) sample). An increase in the amine loading led to a dramatic decrease in the pore volume that was accessible to the nitrogen gas in the volumetric experiment and resulted in 61% of blocking for micro-AC-TETA(30). Loading of larger volumes of amine onto micro-AC resulted in practically complete pore blocking. The values of surface area and total pore volume for micro-AC-TETA(50) and micro-AC-TETA(70) samples are remarkably similar, suggesting, as discussed above, that the impregnating of the microporous material resulted in complete enveloping of the porous particles and blocking the pores without penetrating into all the deeper internal pore space.

Thus, the general scenario of impregnation of micro-AC material with TETA suggests that a significant part of the available pore volume is blocked instead of being filled, i.e. the amine first occupies the outer layer of the micropores in the micro-AC particles and does not penetrate into the deeper internal pore space.

With meso-AC material there was a gradual decrease in the surface area and pore volume as more amine was loaded onto the material (Table 1). In contrast to the micro-AC case only a small level of pore blocking was observed through the whole range of amine loading, with a maximum pore blocking value of 21% for meso-AC-TETA(30) (Fig.3b).

DFT analysis of adsorption isotherms for both kinds of studied materials indicates that the normalized micropore volume available for nitrogen adsorption drops faster than the mesopore volume with an increase of the amine loading (Table 2). It can be seen that $V_{micro} > V_{meso}$ for the micro-AC series (except micro-AC-TETA(50) and micro-AC-TETA(70) where the pore volume is negligible) and $V_{micro} < V_{meso}$ for all loadings of the meso-AC series.

For mostly micro-AC, in agreement with the pore blocking model, there is a sharp initial drop in the accessible micropores with increasing TETA loading from 0 to 30%, where the difference between V_{free} and V_{meas} was largest. With an increase of amine loading from 50% to 70% the relative volume of available micropores tends to zero, and the difference between V_{meas} and V_{free} decreases, indicating that an excess of amine is located on the outer surface of the micro-AC particles. With meso-AC, DFT pore volume analysis calculates a three times reduction in the available micropore volume for 10% of amine loading, and there is no measured micropore volume at higher amine loadings. This may suggest that the initial adsorption of amine results in some of the micropore content being blocked. In the case of meso-AC there is less of a contribution from pore blockage and

the amine distributes more evenly throughout the material, filling the small mesopores first. The latter assumption concerning the predominant filling/blocking of small pores is supported by PSD analysis of the TETA impregnated meso-AC series, where the minimal mesopore size is shifted from <2.5 nm for the original meso-AC material to 4.5 nm for the meso-AC TETA(50) and meso-AC TETA(70) species (Fig. 4).

All these findings imply that in the case of the wet impregnation procedure when small polyamine species are used, the amine molecules form droplet-like aggregates which do not penetrate deep inside the micropores. With an increase of amine loading the impregnating amine forms a continuous layer on the carbon surface and fills the mesopores. Thus, to ensure a more homogeneous distribution of amine across the surface of the material, supports with mesoporous structure are preferential.

3.2 Comparison of different amines at low loadings. EDA, DETA, TETA, PEI600

In order to check the proposed impregnation scenario we have studied the surface properties of micro-AC and meso-AC materials impregnated with a few polyamines of different size but with the same general formula $H-(NH-CH_2CH_2)_n-NH_2$: ethylenediamine (EDA, n=1), diethylenetriamine (DETA, n=2), triethylenetetramine (TETA, n=3) and branched polyethyleneimine with average molecular weight of 600 Da (PEI600, n=13-14). The molecular volumes of amines obtained from liquid densities, along with the calculated volumes and the adsorption cross sectional areas of the amines are shown in Table 3.

Impregnation of micro-AC material with 10% loading of different polyamines (EDA, DETA and PEI-600) showed results that were similar to those observed for micro-AC-TETA(10) (Fig. 5), i.e. all the materials exhibited Type I nitrogen adsorption isotherms, and pore blocking values varied in the range 0-7.5%. The pore blocking values for micro-AC-DETA(10) and micro-AC-TETA(10) samples were calculated to be 7.5 and 5% respectively. The low value of pore blocking for micro-AC-EDA(10) sample is due to the difficulty encountered in controlling the amount of EDA in the sample. EDA has a relatively high vapour pressure and was evaporated during the regeneration step prior to the N_2 adsorption measurement. The low value of pore blocking for the micro-AC-PEI600(10) sample cannot be explained by amine leaching as in the case of lower molecular weight amines, and thus required further elucidation. Therefore a series of the micro-AC samples impregnated with an amine weight loading of 30% were prepared and studied.

An increase of amine loading leads to a significant difference in N_2 adsorption behaviour between the micro-AC species impregnated with lower molecular weight amines (EDA, DETA and TETA) and the micro-AC impregnated with PEI-600. For lower amines the blocking values were in the range 40-60% (Table 1). The trend in the change of the pore blocking values shows that the impregnation with EDA and DETA provides slightly less pore blocking than TETA. The higher value of pore blocking for micro-AC-EDA(30) in comparison to micro-AC-DETA(30) is likely to be the result of the different regeneration conditions used (see section 2.3).

In contrast to the case of micro-AC impregnation with smaller amines, micro-AC-PEI600(30) showed a pore blocking value of only 11%. This agrees with the results of low pore blocking observed for micro-AC-PEI600(10).

The calculated cross-sectional surface areas of the amines used are 27 $Å^2$ for EDA, 45.5 $Å^2$ for DETA, 70 $Å^2$ for TETA and 116.5 $Å^2$ for PEI600 (which is equivalent to a diameter of ~1.2 nm for the spherical conformation of the PEI600 molecule). According to PSD in the original micro-AC material, 75% of the available volume is due to pores with diameters <1.25 nm. Thus, as discussed for impregnation of micro-AC with TETA, the lower amines (EDA, DETA and TETA) can fill the pores on the outer surface of the micro-AC particles and do not penetrate deeper inside the micropores. In contrast, PEI molecules are larger and do not fit into the majority of the pores on the outer micro-AC particle surface, thus leaving micropores still available for nitrogen adsorption.

Impregnation of the meso-AC material with 10% of amine resulted in materials with very similar adsorption properties (Fig. 6), with similar pore blocking values of 10 -13.5 % except for the EDA case. Similar to the case of micro-AC-EDA(10), the pore blocking value of 3% for meso-AC-EDA(10) could be a consequence of the regeneration regime used (40 °C/<1mbar), which may have led to a partial evaporation of amine.

Therefore, for microporous species the size of the amine is critical for successfully loading the support. In the case of meso-AC very little difference was observed on loading the different polyamines onto the carbon support as all molecules can fit into the mesoporous pores.

3.3 Ranking of impregnated materials as candidates for CO_2 adsorbents

The CO_2 capture was studied first on both microporous and mesoporous carbon materials with various TETA loadings. Due to leaching of TETA from the support during cyclic experiments at 75 °C

(not observed during vacuum regeneration for N_2 adsorption measurements) the investigations were then extended to carbons loaded with PEI600.

The temperature dependence of the adsorption process was investigated by performing an adsorption/desorption cycle on two different materials at three different temperatures. The CO_2 adsorption curves for the unmodified micro-AC support are shown in Fig 7a. The trend in the capacity (*q*) with temperature follows the trend of a physisorption process with a decrease in *q* for an increase in temperature. In contrast, from Fig 7b it can be seen that there was a minimum energy requirement for the chemical reaction between the amine and CO_2 to occur. At all temperatures, there was a fast initial uptake of CO_2 followed by a second slower process. At the lower temperatures of 35 °C and 50 °C the kinetics of the reaction/ transport to the active sites was slow (Fig 7b). This resulted in the equilibrium capacity not being reached over the 5 hour timescale of the experiment. The optimum (highest) CO_2 capacity within the timescale of the experiment was observed at 75 °C. However, at this temperature, significant leaching of amine from the carbon support was observed over the course of the experiment. From the TGA-DSC experiment the heat of adsorption (ΔH_{ADS}) and the heat of desorption (ΔH_{DES}) of the process could also be calculated from the heat flow, measured by the DSC using equation 4. Here *m* is the amount of adsorbed CO_2 in moles and *t* is time in seconds.

$$\Delta H = \frac{\int_{t_0}^{t} Heat\ flow\ dt}{m_t - m_{t_0}} \quad \text{(eq. 4)}$$

Processes with values of ΔH that are less than 50 kJ mol^{-1} are considered to be physisorption and values that are greater than 50 kJ mol^{-1} are considered to be chemisorption [15].The values of ΔH_{ADS} and ΔH_{DES}, for the unmodified carbon support were approximately ±28 kJ mol^{-1}, at all the temperatures measured. This clearly indicated that the uptake mechanism was a physisorption process. All the impregnated materials measured had a calculated heat of adsorption of around 90 ± 10 kJ mol^{-1} (Table 4). The calculated values of ΔH_{ADS} and ΔH_{DES} were in agreement to within ±2 kJ mol^{-1}. Examples of experimental heatflow curves can be seen in section 3.4. It was concluded that a chemisorption process was the dominating mechanism of adsorption for the impregnated materials.

To investigate the relationship between the amine loading and the CO_2 capacity of the materials, a range of samples were tested at 75 °C. It can be seen in Table 5 that there was a significant improvement in the CO_2 capacity for all materials loaded with amine compared to the unmodified carbon support. For the micro-AC material there appears to be an optimum loading of amine that achieves the maximum CO_2 capacity per unit mass of adsorbent. As discussed earlier this is likely to

be a consequence of pore blockage and transport limitations of the CO_2 in accessing the active sites for higher loadings.

Fig 8 shows a comparison between the CO_2 uptake at 75 °C for various amine-loaded carbons. It can be seen for both the micro-AC and meso-AC supports that as a larger amount of amine is loaded onto the support there is an increase in the uptake of CO_2. For micro-AC this is true up to an optimal loading point beyond which there is a drop in the CO_2 uptake. In this material the pores are partly filled with amine and it would appear that transport of the CO_2 to all the active sites was limited. With the higher loaded micro-ACs (micro-AC-TETA(50), micro-AC-TETA(75)) it was clear that over the course of the 5 hour experiment an equilibrium state had not been reached between the gas phase and the adsorbed phase. The materials were still adsorbing CO_2. The fast initial uptake was attributed to the fast interaction between the CO_2 and the readily accessible active sites of the amine on the surface. As micro-AC-TETA(50) and micro-AC-TETA(75) have very low BET surface area it is reasonable to assume that the number of active sites exposed directly to the CO_2 in the gas phase is low. We can hypothesize that the second, slower stage of the adsorption process, is a result of the reduction in concentration of available amino groups in the outer layer of amine and there is slow transport of the CO_2 through this layer to the available active sites provided by the amine in the internal pores. Alternatively this could be a secondary reaction between the basic groups and the CO_2, e.g. urea formation[44-46], however determining the details of this reaction does not fall within the scope of the current study.

To estimate how efficiently the amine loaded onto the carbon support was being utilized, the ratio between the moles of CO_2 molecules adsorbed per gram, $q(CO_2)$, and the number of moles of amino groups present in the support per gram, mol(N), was calculated. Primary, secondary and tertiary amine groups are all present in the TETA and PEI600 that were used. The generally accepted interactions between CO_2 and amino groups with and without water present are shown in Fig 9.

In a dry process two amino groups are required to interact with one CO_2 molecule. As a dry gas stream was used in these experiments then in order for the number of amino groups to correspond to the number of active sites available for reaction with CO_2, the value of mol(N) should be halved. Therefore, a value of one for [$q(CO_2)$: (0.5* mol(N))] would correspond to the maximum loading of the CO_2 on the adsorbent by the proposed mechanism. It can be seen in Table 5 that for the micro-AC material the ratio [$q(CO_2)$: 0.5* mol(N)] is low. This implies that the active sites were not being used efficiently for carbon capture. It should be noted that if further time was given for the equilibrium point to be reached then the efficiency of site utilization would increase. However, the

time for the experiment is already relatively long and this further capacity could not be practically utilized in an industrial carbon capture process.

In the case of the meso-AC loaded with TETA, there was an observed increase in CO_2 uptake as the loading increased. Compared to the micro-AC material the overall uptake of CO_2 for comparative loading of TETA was higher in all cases. As discussed earlier the average pore size in meso-AC is larger than in micro-AC and hence a larger number of amine active sites were accessible on the surface for CO_2 adsorption. This resulted in a more significant CO_2 uptake and a more efficient utilization of the available CO_2 active sites as shown in Table 5. The active sites become less accessible to the CO_2 as the amine loads onto the surface of the carbon in multiple layers. However, the amine is more efficiently utilized in all the meso-AC material than in the micro-AC materials.

As can be seen in Table 5, the primary factor in the CO_2 capacity is the amount of loaded amine on the substrate despite a significant decrease in available surface area and pore volume. However, the structure of the support is also important in providing a favourable distribution of the amine across the support surface.

Throughout regeneration and the CO_2 measurement it was apparent that TETA was leaching from the support. This effect was highlighted further by meso-AC-TETA(50) where a second run of the experiment was performed, shown in Fig 8b, a significant drop in the uptake capacity of 20 % was observed in the second cycle. Alongside amine leaching it is possible that the active sites are deactivating through the formation of carboxylate/carbamate/urea species. This effect was investigated by Tanthana et al.[22] through an infra-red spectroscopy study. The rate of amine leaching was lower at lower loadings. This was likely to be a result of more favourable surface interactions between the TETA and the carbon support, than between TETA molecules. As follows from Fig. 4, smaller pores are filled first, the smaller pores will adsorb the amine more strongly than larger ones. This is discussed in more detail in section 3.4, concerning the cyclic experiments.

During cycling, leaching of TETA from the carbon substrate was observed, this was similar to published results for silicas impregnated with tetraethylenepentamine (TEPA).[47, 48]. For this reason higher molecular weight PEI600 was tested on the carbon support at various loadings. As can be seen in Fig. 8c and Table 5 the trend in the CO_2 adsorption uptake is similar to that of the TETA loaded substrates. However, the ratio $q(CO_2)$: [0.5*mol(N)] is lower than in the case of TETA. This was to be expected as PEI600 is a larger molecule, with more sterically hindered amino groups, and is hence less reactive with CO_2. There is therefore a trade-off between the stability of the amine on the carbon support and the reactivity towards the CO_2 gas.

3.4 CO₂ cyclic adsorption experiments

In order to assess the potential of the impregnated materials over several adsorption desorption steps, cyclic experiments were carried out on two materials. meso-AC-TETA(30) was selected, as during the earlier single cycle measurements the leaching of TETA from the carbon support was lower than for TETA-50 and 75 and it had a higher capacity than meso-AC-TETA(10). meso-AC-PEI600(100) was subjected to a cyclic test as it had the highest capacity of the materials impregnated with polyethyleneimine. The experiments were conducted at 75 °C over 16 hours with 4 adsorption and 4 desorption cycles. As shown in Fig 10a meso-AC-PEI600(100) was stable over the 4 ADS/DES cycles. There was a CO_2 uptake of 1.22 mmol g^{-1} and a reproducible heat flow for each ADS/DES cycle. In the case of meso-AC-TETA(30) (Fig 10b) there was a slow leaching of TETA from the support. This resulted in a reduced uptake of 9 % between the 1st and 4th adsorption cycle. This degradation in the material means that it would have to be regularly replaced if it was used in a carbon capture process. As a result the support impregnated with the heavier PEI600 is more suitable despite the less efficient utilization of the NH sites.

4. Conclusions

The structural properties of two different types (microporous and mesoporous) of porous carbon materials were studied as supports for impregnation with low molecular weight polyamines by volumetric nitrogen adsorption. Microporous materials showed that there was a tendency for some of the free pore volume to be inaccessible (blocked) for nitrogen adsorption even at a low weight loading of polyamines. Mesoporous materials in contrast appeared to be more suited to impregnation with polyamines with a low level of blocked pore volume.

A series of materials, were tested under CO_2 partial pressure conditions that are similar to that of the flue gas of a fossil fuel power plant. On the addition of polyamines to both types of the raw carbon material the adsorption mechanism changed from a physisorption to a chemisorption process. All impregnated materials tested exhibited an enhanced affinity towards CO_2. The relative improvements compared to the starting micro-AC are highlighted in Fig.11.

It was apparent that the value of the CO_2 capacity was dependent on the structure of the carbon support, the amount of loaded amine and the type of amine. It was hypothesized that better mass transport to the active sites was possible when the material loaded had larger mesopores as opposed to small micropores, where access to the active sites in the inner pores was easily hindered.

For micro-AC there was an optimum amine loading beyond which the CO_2 capacity was lower. In the case of the meso-AC series there was a gradual increase in the CO_2 capacity as a larger amount of amine was loaded onto the support. It can be concluded that microporous supports are not ideal candidates for impregnation with amines. This is supported by the mixed results achieved by those attempting such work in the literature [11, 29]. It was suggested that as a greater volume of amine was loaded onto the carbon support, transport to the active sites was limited due to a blocking effect where the CO_2 had difficulty accessing the active sites. These findings support the conclusions from recent studies of PEI impregnated silica materials. [25]

The efficiency of the reaction of CO_2 with amine was relatively constant within each meso-AC and micro-AC series. However, the TETA impregnated meso-AC series interacted more efficiently with CO_2 (*ca.* 0.4 CO_2 molecules per 2 nitrogen atoms) compared to the micro-AC-TETA series (*ca.* 0.2 CO_2 molecules per 2 nitrogen atoms). It was also observed that at the same mass loading, smaller polyamines (TETA) are more reactive towards CO_2 than the larger less volatile alternatives (PEI600), i.e. the efficiency of amino group utilization in the meso-AC-TETA series is higher than for the meso-AC-PEI600 series. However, there was a pay-off in terms of stability and at high loading a drastic drop off in capacity was observed from the first to subsequent capture/regeneration cycles.

5. References

[1] C.-H. Yu, C.-H. Huang, C.-S. Tan, A Review of CO2 Capture by Absorption and Adsorption, Aerosol and Air Quality Research, 12 (2012) 745 - 769.

[2] J.M. Dias, M.C.M. Alvim-Ferraz, M.F. Almeida, J. Rivera-Utrilla, M. Sánchez-Polo, Waste materials for activated carbon preparation and its use in aqueous-phase treatment: A review, Journal of Environmental Management, 85 (2007) 833-846.

[3] S.A. Dastgheib, T. Karanfil, W. Cheng, Tailoring activated carbons for enhanced removal of natural organic matter from natural waters, Carbon, 42 (2004) 547-557.

[4] D. Soares Maia, J.C.A. de Oliveira, J. Toso, K. Sapag, R. López, D.S. Azevedo, C. Cavalcante, Jr., G. Zgrablich, Characterization of the PSD of activated carbons from peach stones for separation of combustion gas mixtures, Adsorption, 17 (2011) 853-861.

[5] H. Marsh, F. Rodríguez-Reinoso, Chapter 8 - Applicability of Activated Carbon, in: H. Marsh, F. Rodríguez-Reinoso (Eds.) Activated Carbon, Elsevier Science Ltd, Oxford, 2006, pp. 383-453.

[6] S. Choi, J.H. Drese, C.W. Jones, Adsorbent Materials for Carbon Dioxide Capture from Large Anthropogenic Point Sources, ChemSusChem, 2 (2009) 796-854.

[7] N. Mohamad Nor, L.C. Lau, K.T. Lee, A.R. Mohamed, Synthesis of activated carbon from lignocellulosic biomass and its applications in air pollution control—a review, Journal of Environmental Chemical Engineering, 1 (2013) 658-666.

[8] M. Balsamo, T. Budinova, A. Erto, A. Lancia, B. Petrova, N. Petrov, B. Tsyntsarski, CO2 adsorption onto synthetic activated carbon: Kinetic, thermodynamic and regeneration studies, Separation and Purification Technology, 116 (2013) 214-221.

[9] C.S. Lee, Y.L. Ong, M.K. Aroua, W.M.A.W. Daud, Impregnation of palm shell-based activated carbon with sterically hindered amines for CO2 adsorption, Chem. Eng. J. (Amsterdam, Neth.), 219 (2013) 558-564.

[10] M. Maroto-Valer, Z. Lu, Y. Zhang, Z. Tang, Sorbents for CO2 capture from high carbon fly ashes, Waste Management, 28 (2008) 2320-2328.

[11] J. Wang, H. Chen, H. Zhou, X. Liu, W. Qiao, D. Long, L. Ling, Carbon dioxide capture using polyethylenimine-loaded mesoporous carbons, Journal of Environmental Sciences, 25 (2013) 124-132.

[12] C.S. Watana Kangwanwatanaa, Paitoon Tontiwachwuthikul, Study of CO2 Adsorption Using Adsorbent Modified with Piperazine, Chemical Engineering Transactions, 35 (2013) 403-408.

[13] Z. Chen, S. Deng, H. Wei, B. Wang, J. Huang, G. Yu, Activated carbons and amine-modified materials for carbon dioxide capture — a review, Front. Environ. Sci. Eng., 7 (2013) 326-340.

[14] A. Boonpoke, S. Chiarakorn, N. Laosiripojana, S. Towprayoon, A. Chidthaisong, Investigation of CO2 adsorption by bagasse-based activated carbon, Korean J. Chem. Eng., 29 (2012) 89-94.

[15] A. Samanta, A. Zhao, G.K.H. Shimizu, P. Sarkar, R. Gupta, Post-Combustion CO2 Capture Using Solid Sorbents: A Review, Industrial & Engineering Chemistry Research, 51 (2011) 1438-1463.

[16] W.-J. Son, J.-S. Choi, W.-S. Ahn, Adsorptive removal of carbon dioxide using polyethyleneimine-loaded mesoporous silica materials, Microporous and Mesoporous Materials, 113 (2008) 31-40.

[17] E.S. Sanz-Pérez, M. Olivares-Marín, A. Arencibia, R. Sanz, G. Calleja, M.M. Maroto-Valer, CO2 adsorption performance of amino-functionalized SBA-15 under post-combustion conditions, International Journal of Greenhouse Gas Control, 17 (2013) 366-375.

[18] M.A. Alkhabbaz, R. Khunsupat, C.W. Jones, Guanidinylated poly(allylamine) supported on mesoporous silica for CO2 capture from flue gas, Fuel, 121 (2014) 79-85.

[19] G. Qi, Y. Wang, L. Estevez, X. Duan, N. Anako, A.-H.A. Park, W. Li, C.W. Jones, E.P. Giannelis, High efficiency nanocomposite sorbents for CO2 capture based on amine-functionalized mesoporous capsules, Energy & Environmental Science, 4 (2011) 444-452.

[20] X. Xu, C. Song, J.M. Andresen, B.G. Miller, A.W. Scaroni, Preparation and characterization of novel CO2 'molecular basket' adsorbents based on polymer-modified mesoporous molecular sieve MCM-41, Microporous and Mesoporous Materials, 62 (2003) 29-45.

[21] M.U. Thi Le, S.-Y. Lee, S.-J. Park, Preparation and characterization of PEI-loaded MCM-41 for CO_2 capture, International Journal of Hydrogen Energy, 39 (2014) 12340-12346.

[22] J. Tanthana, S.S.C. Chuang, In Situ Infrared Study of the Role of PEG in Stabilizing Silica-Supported Amines for CO_2 Capture, ChemSusChem, 3 (2010) 957-964.

[23] R. Sanz, G. Calleja, A. Arencibia, E.S. Sanz-Pérez, CO_2 adsorption on branched polyethyleneimine-impregnated mesoporous silica SBA-15, Applied Surface Science, 256 (2010) 5323-5328.

[24] D.J.N. Subagyono, M. Marshall, G.P. Knowles, A.L. Chaffee, CO_2 adsorption by amine modified siliceous mesostructured cellular foam (MCF) in humidified gas, Microporous and Mesoporous Materials, 186 (2014) 84-93.

[25] D. Wang, X. Wang, X. Ma, E. Fillerup, C. Song, Three-dimensional molecular basket sorbents for CO_2 capture: Effects of pore structure of supports and loading level of polyethylenimine, Catalysis Today, 233 (2014) 100-107.

[26] H.J. Lim, K. Lee, Y.S. Cho, Y.S. Kim, T. Kim, C.R. Park, Experimental consideration of the Hansen solubility parameters of as-produced multi-walled carbon nanotubes by inverse gas chromatography, Physical Chemistry Chemical Physics, 16 (2014) 17466-17472.

[27] C.M. Hansen, Hansen Solubility Parameters: A User's Handbook, 2nd Edition, CRC Press, 2007, ISBN 9780849372483, (2007).

[28] A. Subrenat, J.N. Baléo, P. Le Cloirec, P.E. Blanc, Electrical behaviour of activated carbon cloth heated by the joule effect: desorption application, Carbon, 39 (2001) 707-716.

[29] M.K. Aroua, W.M.A.W. Daud, C.Y. Yin, D. Adinata, Adsorption capacities of carbon dioxide, oxygen, nitrogen and methane on carbon molecular basket derived from polyethyleneimine impregnation on microporous palm shell activated carbon, Separation and Purification Technology, 62 (2008) 609-613.

[30] Z.-l. Liu, Y. Teng, K. Zhang, Y. Cao, W.-p. Pan, CO_2 adsorption properties and thermal stability of different amine-impregnated MCM-41 materials, Journal of Fuel Chemistry and Technology, 41 (2013) 469-475.

[31] A. Grondein, D. Bélanger, Chemical modification of carbon powders with aminophenyl and aryl-aliphatic amine groups by reduction of in situ generated diazonium cations: Applicability of the grafted powder towards CO_2 capture, Fuel, 90 (2011) 2684-2693.

[32] H. Yang, Y. Yuan, S.C.E. Tsang, Nitrogen-enriched carbonaceous materials with hierarchical micro-mesopore structures for efficient CO_2 capture, Chemical Engineering Journal, 185–186 (2012) 374-379.

[33] D.-I. Jang, S.-J. Park, Influence of amine grafting on carbon dioxide adsorption behaviors of activated carbons, Bull. Korean Chem. Soc., 32 (2011) 3377-3381.

[34] Y. Du, Z. Du, W. Zou, H. Li, J. Mi, C. Zhang, Carbon dioxide adsorbent based on rich amines loaded nano-silica, Journal of Colloid and Interface Science, 409 (2013) 123-128.

[35] A. Houshmand, M.S. Shafeeyan, A. Arami-Niya, W.M.A.W. Daud, Anchoring a halogenated amine on the surface of a microporous activated carbon for carbon dioxide capture, Journal of the Taiwan Institute of Chemical Engineers, 44 (2013) 774-779.

[36] K. Böhme, W.-D. Einicke, O. Klepel, Templated synthesis of mesoporous carbon from sucrose—the way from the silica pore filling to the carbon material, Carbon, 43 (2005) 1918-1925.

[37] J.P. Toso, J.C.A. Oliveira, D.A. Soares Maia, V. Cornette, R.H. López, D.C.S. Azevedo, G. Zgrablich, Effect of the pore geometry in the characterization of the pore size distribution of activated carbons, Adsorption, 19 (2013) 601-609.

[38] M. Thommes, K.A. Cychosz, A.V. Neimark, Chapter 4 - Advanced Physical Adsorption Characterization of Nanoporous Carbons, in: J.M.D. Tascón (Ed.) Novel Carbon Adsorbents, Elsevier, Oxford, 2012, pp. 107-145.

[39] J. Landers, G.Y. Gor, A.V. Neimark, Density functional theory methods for characterization of porous materials, Colloids and Surfaces A: Physicochemical and Engineering Aspects, 437 (2013) 3-32.

[40] G. Socrates, Infrared and Raman Characteristic Groups Frequencies: Tables and Charts. Third Edition, John Wiley & Sons, Ltd, ISBN 0-471-85298-8, (2001).

[41] K.S.W. Sing, D.H. Everett, R.A.W. Haul, L. Moscou, R.A. Pierotti, J. Rouquerol, T. Siemieniewska, Reporting physisorption data for gas solid systems with special reference to the determination of surface-area and porosity (recommodations 1984), Pure and Applied Chemistry, 57 (1985) 603-619.

[42] E. Jo, Y.H. Jhon, S.B. Choi, J.-G. Shim, J.-H. Kim, J.H. Lee, I.-Y. Lee, K.-R. Jang, J. Kim, Crystal structure and electronic properties of 2-amino-2-methyl-1-propanol (AMP) carbamate, Chemical Communications, 46 (2010) 9158-9160.

[43] R. Sanz, G. Calleja, A. Arencibia, E.S. Sanz-Pérez, Amino functionalized mesostructured SBA-15 silica for CO2 capture: Exploring the relation between the adsorption capacity and the distribution of amino groups by TEM, Microporous and Mesoporous Materials, 158 (2012) 309-317.

[44] H. Ogura, K. Takeda, R. Tokue, T. Kobayashi, A Convenient Direct Synthesis of Ureas from Carbon Dioxide and Amines, Synthesis, 1978 (1978) 394-396.

[45] C.-C. Tai, M.J. Huck, E.P. McKoon, T. Woo, P.G. Jessop, Low-Temperature Synthesis of Tetraalkylureas from Secondary Amines and Carbon Dioxide, The Journal of Organic Chemistry, 67 (2002) 9070-9072.

[46] A. Sayari, Y. Belmabkhout, Stabilization of Amine-Containing CO2 Adsorbents: Dramatic Effect of Water Vapor, Journal of the American Chemical Society, 132 (2010) 6312-6314.

[47] J.C. Hicks, J.H. Drese, D.J. Fauth, M.L. Gray, G. Qi, C.W. Jones, Designing Adsorbents for CO2 Capture from Flue Gas-Hyperbranched Aminosilicas Capable of Capturing CO2 Reversibly, Journal of the American Chemical Society, 130 (2008) 2902-2903.

[48] C. Chen, S.-T. Yang, W.-S. Ahn, R. Ryoo, Amine-impregnated silica monolith with a hierarchical pore structure: enhancement of CO2 capture capacity, Chemical Communications, (2009) 3627-3629.

Table 1: Overview of surface properties of the studied materials

Sample name	BET surface area (m^2/g)	Pore volume (cc/g) NLDFT (slit/cyl)			V_{carbon}* (cc/g)	V_{amine}** (cc/g)	$V_{free} = V_{carbon} - V_{amine}$ (cc/g)***	blocked volume, %****
		Total (V_{meas})	Micro (<2 nm)	Meso (>2 nm)				
micro-AC	1336	0.68	0.59	0.085	0.68	0	0.68	0
micro-AC-TETA(10)	954	0.50	0.42	0.079	0.61	0.093	0.52	5
micro-AC-TETA(30)	220	0.11	0.093	0.018	0.52	0.24	0.28	61
micro-AC-TETA(50)	24	0.017	0.007	0.010	0.45	0.34	0.11	85
micro-AC-TETA(70)	7	0.014	0	0.014	0.40	0.42	-0.022	-
micro-AC-EDA(10)	1022	0.53	0.43	0.094	0.61	0.10	0.51	-2
micro-AC-DETA(10)	938	0.48	0.38	0.097	0.61	0.095	0.52	7.5
micro-AC-PEI600(10)	1017	0.53	0.45	0.076	0.61	0.087	0.53	0
micro-AC-EDA(30)	265	0.14	0.09	0.043	0.52	0.26	0.26	48
micro-AC-DETA(30)	318	0.17	0.11	0.060	0.52	0.24	0.28	41
micro-AC-PEI600(30)	519	0.27	0.20	0.065	0.52	0.22	0.30	11
meso-AC	817	1.1	0.086	0.98	1.1	0	1.1	0
meso-AC-TETA(10)	510	0.75	0.029	0.72	0.97	0.093	0.87	14
meso-AC-TETA(30)	274	0.46	0	0.46	0.82	0.24	0.58	20
meso-AC-TETA(50)	162	0.30	0	0.30	0.71	0.34	0.37	18
meso-AC-TETA(70)	93	0.19	0	0.19	0.62	0.42	0.21	9
meso-AC-EDA(10)	589	0.84	0.051	0.79	0.97	0.10	0.87	3
meso-AC-DETA(10)	518	0.77	0.028	0.74	0.97	0.095	0.87	12
meso-AC-PEI600(10)	541	0.79	0.024	0.77	0.97	0.087	0.88	10

*- in impregnated materials the mass fraction of activated carbon was not equal to 100%. Therefore, the pore volume of the carbon per gram of impregnated material (V_{carbon}) is equal to the mass fraction of the carbon support in the composite multiplied by the pore volume per gram of unmodified carbon.

** - the volume of added amine in a gram of impregnated material

*** - see section 3.1 for details

**** - $[1-V_{meas}/(V_{carbon}-V_{amine})]*100\%$, for detail see section 3.1

Table 2: Relative pore volume in the investigated samples (normalized to the volume of micro- and mesopores in original micro-AC/meso-AC materials)

Sample name	V_{micro}/V_{meso} (cc/g)	norm V_{micro}	norm V_{meso}
micro-AC	0.59/0.085	1	1
micro-AC-TETA(10)	0.42/0.079	0.71	0.93
micro-AC-TETA(30)	0.093/0.018	0.16	0.22
micro-AC-TETA(50)	0.007/0.010	0.01	0.12
micro-AC-TETA(70)	0/0.014	0.00	0.17
meso-AC	0.086/0.98	1	1
meso-AC-TETA(10)	0.029/0.72	0.34	0.74
meso-AC-TETA(30)	0/0.46	0.00	0.47
meso-AC-TETA(50)	0/0.30	0.00	0.31
meso-AC-TETA(70)	0/0.19	0.00	0.19

Table 3: Sizes of amine molecules

amine	Molecular volume, (Å^3)*		Calculated cross-sectional surface area, (Å^2)
	from molar volume of liquid	calculated for the given shape using bond lengths/angles & vdW constants	
EDA	111	106, (cylinder l=5.4 Å, d=5 Å)	27
DETA	180	178.5 (cylinder l=9.1 Å, d=5 Å)	45.5
TETA linear (60%)	247.5	250 (cylinder l=12.75 Å, d=5 Å)	64
TETA branched (40%)	248.5	245 (disc d=7.9 Å, h=5 Å)	49
PEI600 branched	950	950 (sphere, d=12.2 Å)	116.5

*Molecular volumes for the molecules were estimated on the basis of their liquid densities. For estimation of areas occupied by polyamines the molecular volumes were calculated for cylindrical (linear species), disc and sphere (for branched species) geometries using the values of bond lengths of 1.53 Å for C-C bond, 1.47 Å for C-N bond, 1.09 Å for C-H bond, 1.01 Å for N-H bond, tetrahedral bond angle of 109º for all bonds and 1.2 Å for van der Waals' radius of hydrogen atom; d stands for diameter, l- length and h - height.

Table 4: Heat of CO_2 adsorption ΔH_{ADS} and ΔH_{DES} of several materials at different temperatures

	Temperature/ °C	$-\Delta H_{ADS}$ kJ mol^{-1}	ΔH_{DES} kJ mol^{-1}
micro-AC	35	28.0	26.2
	50	27.8	26.3
	75	28.5	28.6
micro-AC-TETA(50)	35	97.4	98.0
	50	88.9	88.7
	75	90.9	90.7
	90	90.5	91.1
meso-AC-TETA(30)	75	87.8	85.7
meso-AC-TETA(50)	75	91.2	91.3
meso-AC-PEI600(100)	75	92.5	92.4

Table 5: CO_2 capacities of the materials with various loadings of amine at 75 °C after 5 hours of adsorption. The efficiency of the amine utilization is calculated as the ratio of the moles of CO_2 up taken by the adsorbent to the number of moles of amino groups available for adsorption, $q(CO_2)$: [0.5*mol(N)].

	$q(CO_2)/$ mmol g^{-1}	mol(N)/ mmol g^{-1}	$q(CO_2)$: [0.5*mol(N)]
meso-AC-TETA(10)	0.24	2.49	0.19
meso-AC-TETA(30)	1.15	6.32	0.36
meso-AC-TETA(50)	1.67	9.11	0.37
meso-AC-TETA(50), run 2	1.33	9.11	0.29
meso-AC-TETA(75)	1.85	11.7	0.32
meso-AC-PEI600(20)	0.28	4.05	0.14
meso-AC-PEI600(40)	0.68	6.94	0.20
meso-AC-PEI600(60)	0.98	9.10	0.22
meso-AC-PEI600(75)	1.30	10.4	0.25
meso-AC-PEI600(100)	1.40	12.1	0.23
micro-AC-TETA(10)	0.20	2.49	0.16
micro-AC-TETA(30)	0.57	6.32	0.18
micro-AC-TETA(50)	1.05	9.11	0.23
micro-AC-TETA(65)	0.43	10.8	0.08

Figures:
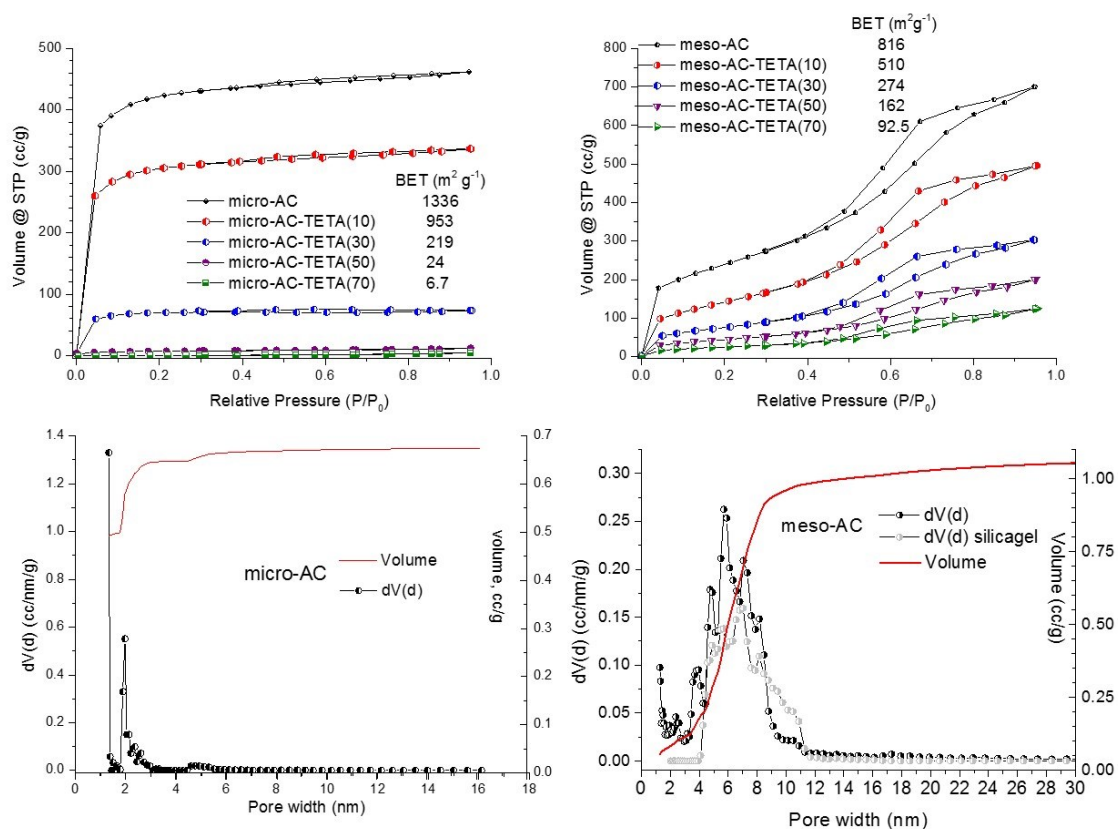
Figure 1: N$_2$ adsorption isotherms and pore size distributions, 77 K. (a) micro-AC impregnated with various weight loadings of TETA. (b) meso-AC impregnated with various weight loadings of TETA (c) Pore size distribution of micro-AC (d) Pore size distribution of meso-AC and silica gel
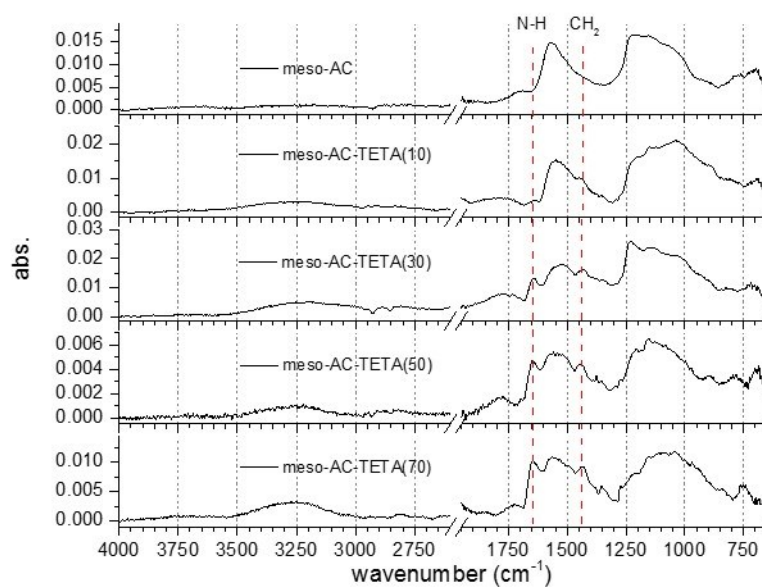
Figure 2: ATR FTIR spectra of the synthesized meso-AC material and meso-AC-TETA impregnated species.
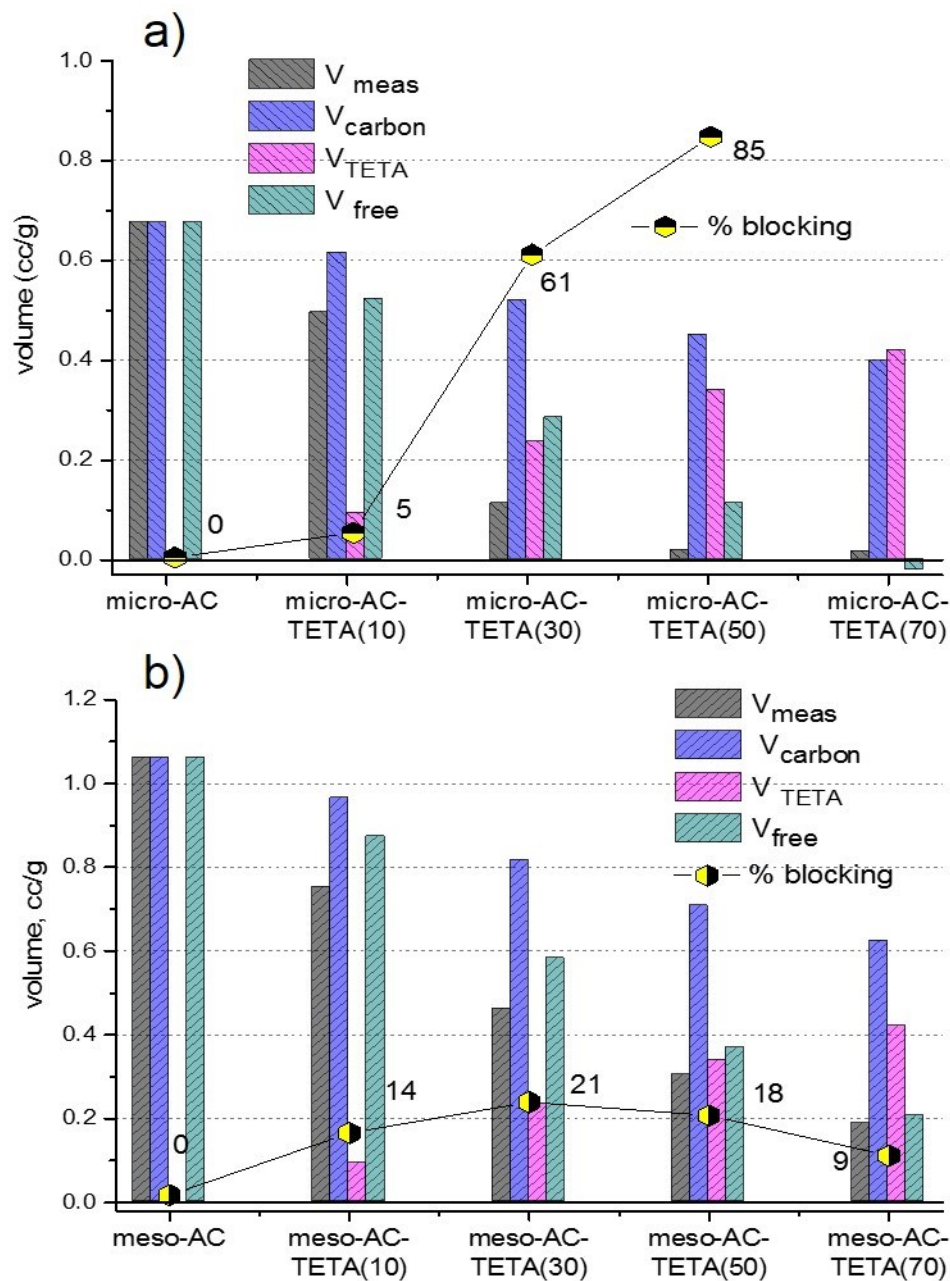
Figure 3: Comparison of the total pore volume of carbons loaded with TETA. (a) micro-AC-TETA series, (b) meso-AC-TETA series. V_{meas} :total pore volume calculated by DFT; V_{carbon} : volume of carbon support taking into account mass fraction of impregnated amine; V_{TETA}: volume of TETA added; V_{free} : expected volume available after impregnation; % blocking: ratio $(V_{free}-V_{meas})/V_{free}$ *100
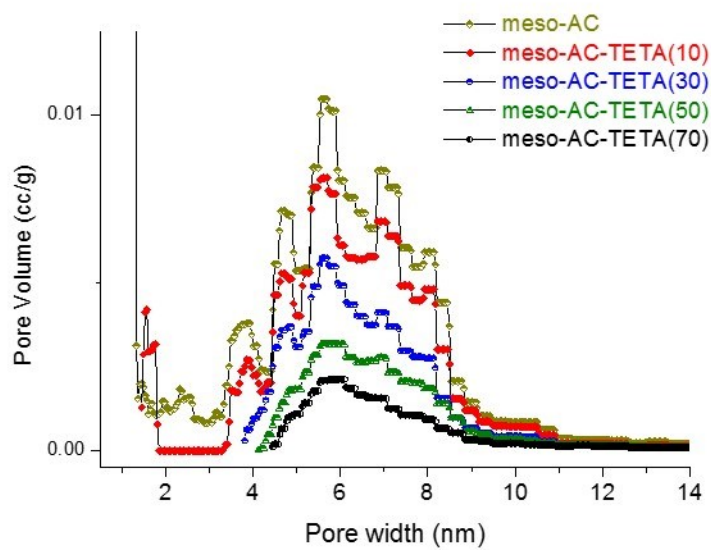
Figure 4: Pore size distribution of meso-AC impregnated with TETA. Calculated using NLDFT pore size distribution analysis.
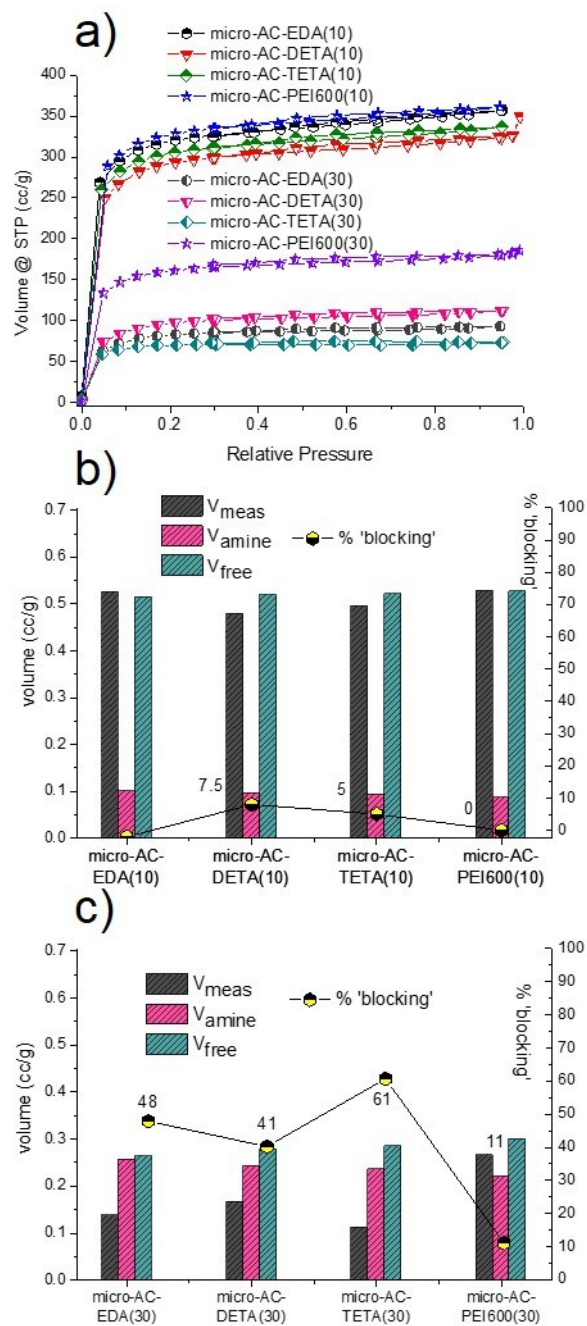
Figure 5: Impregnation of micro-AC with polyamines of different molecular weights. (a) N_2 adsorption isotherms of micro-AC weight loaded with 10 and 30% polyamine. NLDFT determined pore volume (V_{meas}), expected available volume (V_{free}) and % pore blocking for (b) micro-AC-amine(10) and (c) micro-AC-amine(30)
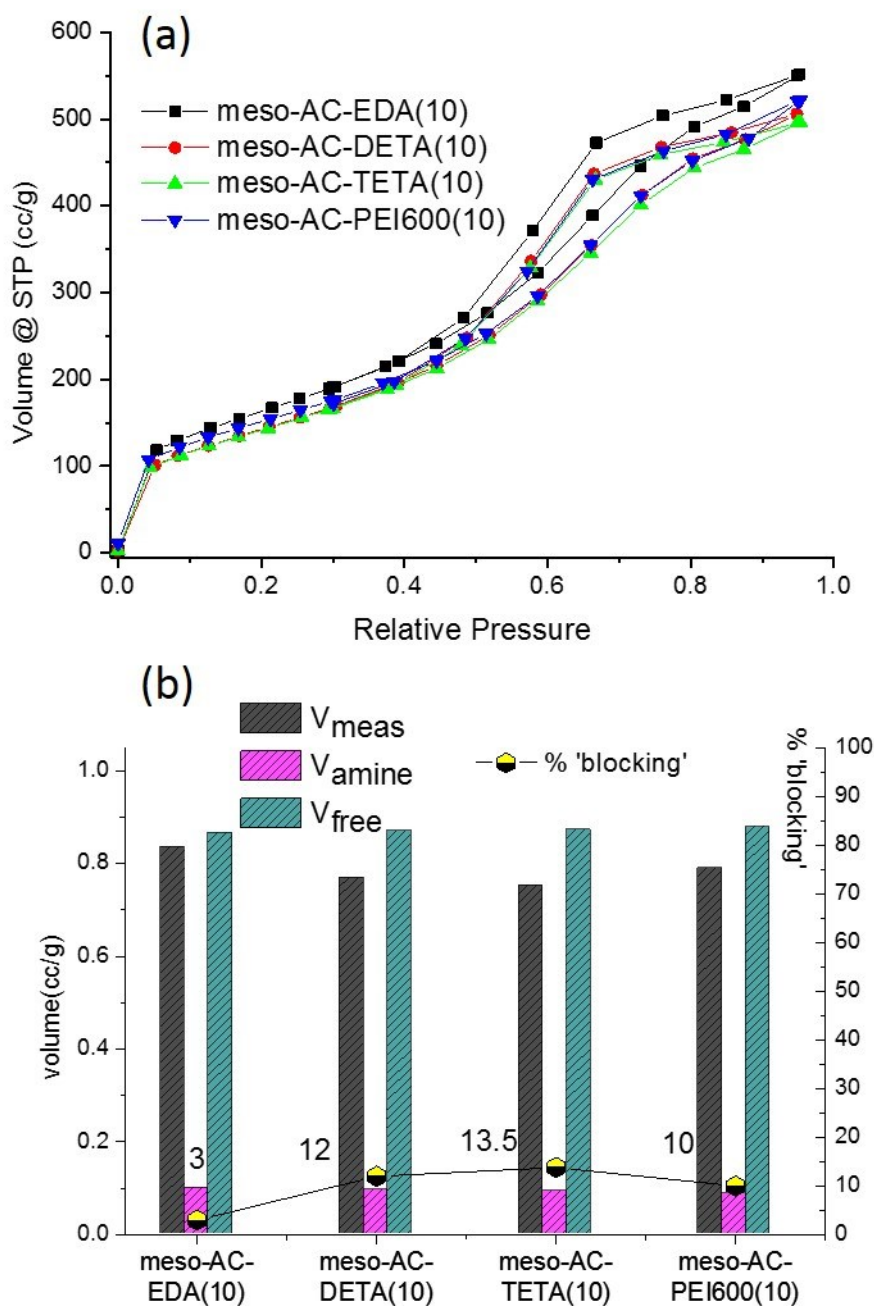
Figure 6: Impregnation of meso-AC with polyamines of different molecular weights. (a) N_2 adsorption isotherms of micro-AC weight loaded with 10%. (b) NLDFT determined pore volume (V_{meas}), expected available volume (V_{free}) and % pore blocking for meso-AC-amine(10)
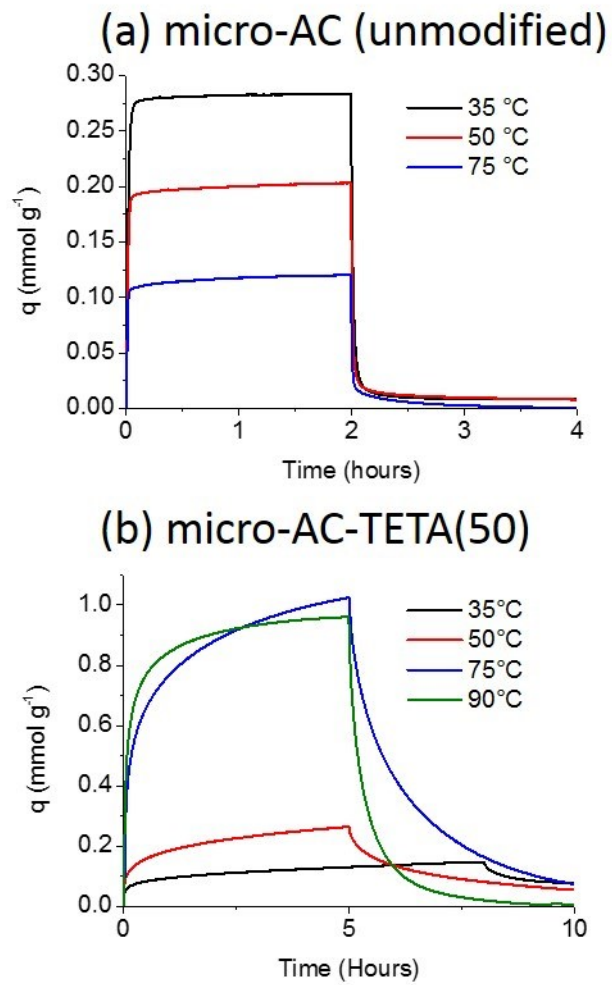
Figure 7: CO_2 uptake curves at various temperatures measured by thermal gravimetric analysis.
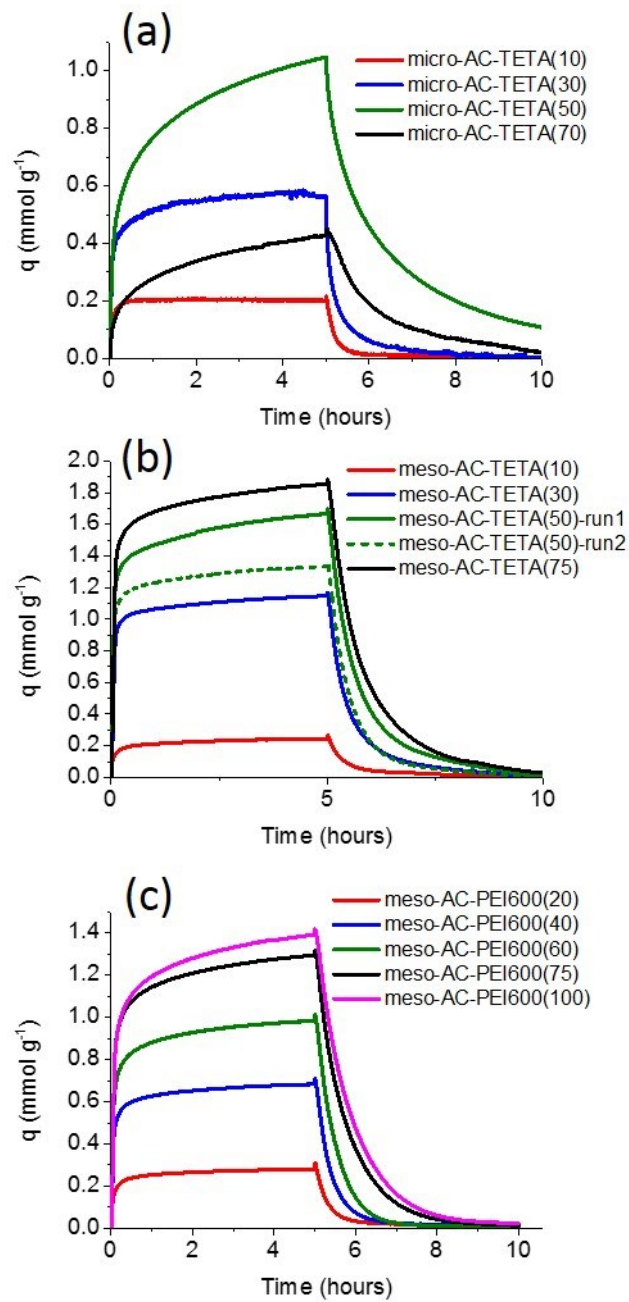
Figure 8: (a) Experimental uptake curves of micro-AC with various loadings of TETA. (b) Experimental uptake curves of meso-AC with various loadings of TETA. (c) TGA uptake curves of meso-AC with various weight loadings of PEI600 Measured at 75 °C, 0.1 bar CO_2, 0.9 bar He.
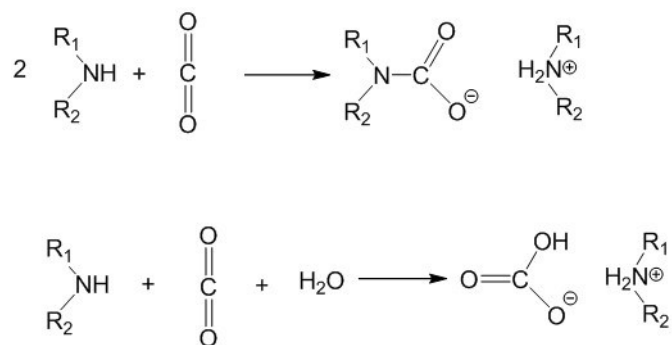
Figure 9: Mechanism of interaction of CO_2 with basic NH groups. Top: Without water present, Bottom: With water present[15]
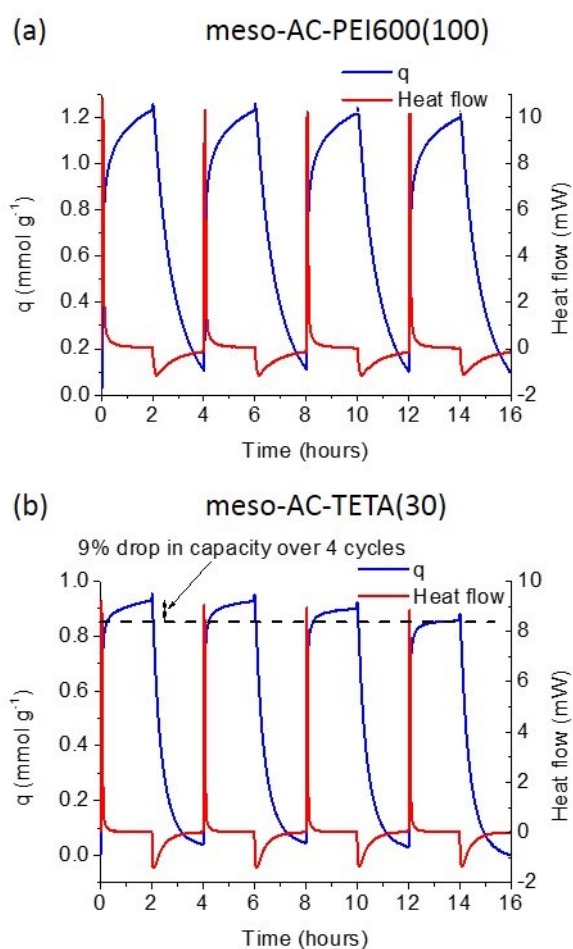
Figure 10: Cyclic experiments- 2 hours adsorption of CO_2 at 0.1 bar, 0.9 bar He, followed by desorption under pure helium flow. Four cycles, flow rate remains constant throughout the experiment. Temperature: 75 °C. (a) meso-AC-PEI600(100), (b) meso-AC-TETA(30)
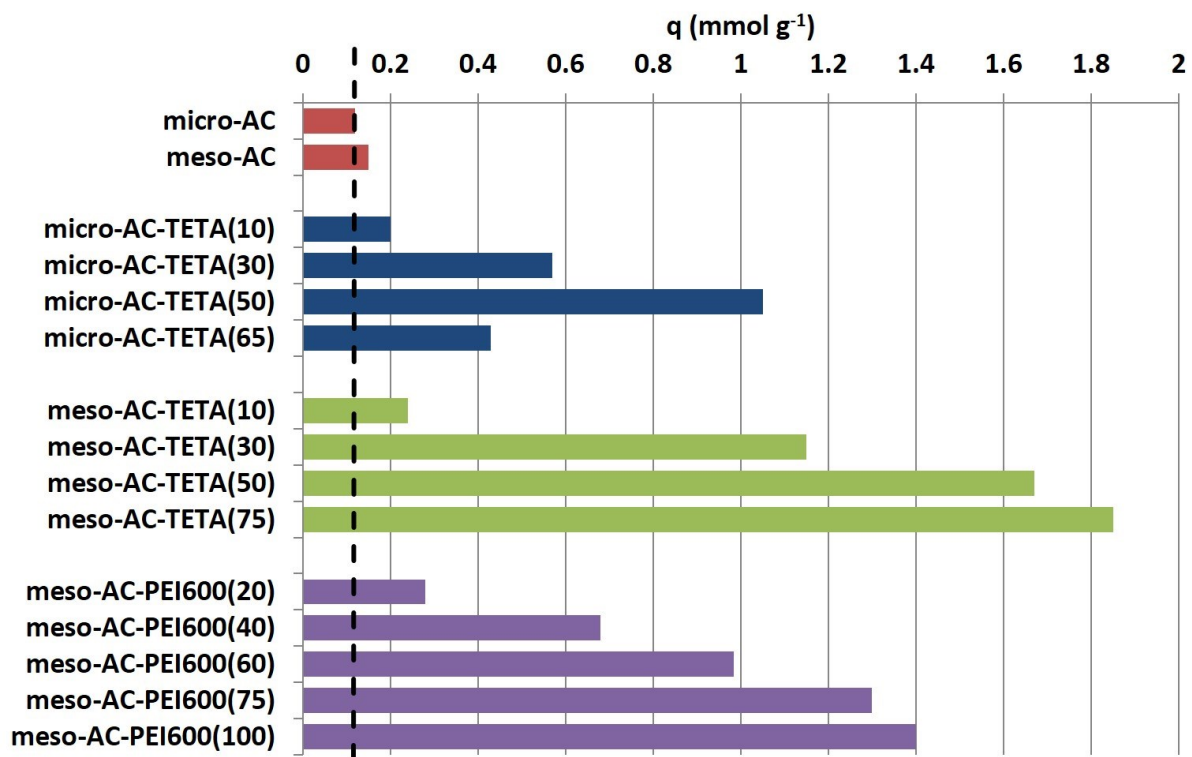
Figure 11: Summary chart showing uptake capacity of micro-AC and meso-AC porous carbons loaded with various quantities of aziridine derivatives.